

Structural Invariance in Silver(I) Coordination Networks Formed Using Flexible Four-Armed Thiopyridine Ligands

David B. Cordes and Lyall R. Hanton*

Department of Chemistry, University of Otago, P.O. Box 56, Dunedin, New Zealand

Received September 28, 2006

Two new isomeric, flexible four-armed thioether pyridine-containing ligands 1,2,4,5-tetrakis(3-pyridylmethylsulfanyl-methyl)benzene (**3tet**) and 1,2,4,5-tetrakis(4-pyridylmethylsulfanyl-methyl)benzene (**4tet**) were prepared and characterized. The ligand **3tet** gave rise to three isomorphous 3-D networks when reacted with AgClO_4 (**1**), AgPF_6 (**2**), and AgCF_3CO_2 (**3**). The topology of the resulting networks was that of the pyrite net. The ligand **4tet** gave rise to two isotopological 3-D networks when reacted with AgClO_4 (**4·2MeCN·2CHCl}_3**) and AgPF_6 (**5·6MeCN**). The topology of these networks was that of the rutile net. A third type of 3-D network of previously unknown topology was formed on reaction with AgCF_3SO_3 (**6·3H}_2\text{O}**). The network showed nodes with short topological terms $4^2.6$ and $4^4.6^2.8^7.10^2$. All six networks were binodal and based on three-connected Ag(I) nodes and six-connected ligand-centered nodes. In all of the networks the flexible ligands **3tet** and **4tet** showed two categories of ligand geometry which in all but one case gave rise to an interligand three-layered π stack. The networks showed a remarkable lack of dependence on the nature of the counterion and solvent.

Introduction

The use of ligands with multiple flexible arms, each containing several donor atoms, presents a number of challenges for the synthesis of coordination polymers, as the flexible portions of the arms do not generally behave in a predictable manner.¹ This problem is further compounded in complexes involving Ag(I) ions where subtle changes in anions or solvents used for crystallization have been seen to lead to significant changes in overall coordination–polymer architecture.² Despite these limits on the controllability of the resulting architectures, the structural diversity that is created allows opportunities to gain a better understanding of the factors that lead to this diversity. One of the ways in which a degree of control has been introduced is through

the concept of facial segregation.³ The most commonly encountered examples of this phenomenon in supramolecular chemistry occur when benzene rings with six substituents adopt an alternating up–down–up–down–up–down pattern relative to the plane of the ring for the six substituents. This has been applied to coordination polymers,⁴ although it has also been found that other effects can override this segregation. Depending on the nature and positioning of the functionality built into an arm, facial segregation can be superseded by the coordination requirements of the donor atoms or metal ion.^{4c} A further number of coordination polymer systems showing facial segregation have also been seen where the ligands used have four flexible arms, rather than six, attached to the benzene ring,⁵ although once again there are exceptions to the rule.⁶

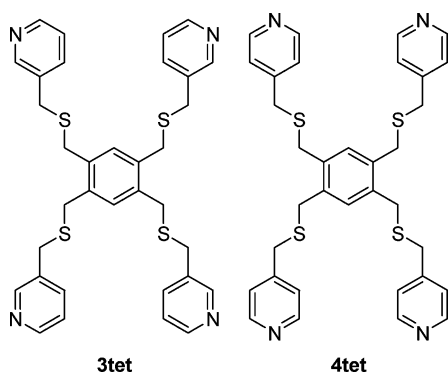
Previous work involving flexible two-armed ligands has led to the synthesis of a number of one-dimensional coordination polymers.⁷ One of the supramolecular motifs seen frequently in the coordination polymers involving these

* To whom correspondence should be addressed. E-mail: lhanton@alkali.otago.ac.nz.

- (1) (a) Yang, X.; Ranford, J. D.; Vittal, J. J. *Cryst. Growth Des.* **2004**, *4*, 781–788. (b) Kumar, V. S. S.; Pigge, F. C.; Rath, N. P. *New J. Chem.* **2003**, *27*, 1554–1556. (c) Moulton, B.; Zaworotko, M. J. *Chem. Rev.* **2001**, *101*, 1629–1658. (d) Moulton, B.; Zaworotko, M. J. *Adv. Supramol. Chem.* **2000**, *7*, 235–283. (e) Hagrman, P. J.; Hagrman, D.; Zubieta, J. *Angew. Chem., Int. Ed.* **1999**, *38*, 2638–2684.
- (2) (a) Eddaoudi, M.; Moler, D. B.; Li, H.; Chen, B.; Reineke, T. M.; O’Keeffe, M.; Yaghi, O. M. *Acc. Chem. Res.* **2001**, *34*, 319–330. (b) Blake, A. J.; Champness, N. R.; Hubberstey, P.; Li, W.-S.; Schröder, M.; Withersby, M. A. *Coord. Chem. Rev.* **1999**, *183*, 117–138. (c) Batten, S. R.; Robson, R. *Angew. Chem., Int. Ed.* **1998**, *37*, 1460–1494.

- (3) Hennrich, G.; Ansllyn, E. V. *Chem. Eur. J.* **2002**, *8*, 2218–2224.
- (4) (a) Ohi, H.; Tachi, Y.; Kunimoto, T.; Itoh, S. *Dalton Trans.* **2005**, 3146–3247. (b) Ohi, H.; Tachi, Y.; Itoh, S. *Inorg. Chem.* **2004**, *43*, 4561–4563. (c) Goodgame, D. M. L.; Grachvogel, D. A.; White, A. J. P.; Williams, D. J. *Inorg. Chim. Acta* **2003**, *344*, 214–220. (d) Hoskins, B. F.; Robson, R.; Slizys, D. A. *Angew. Chem., Int. Ed. Engl.* **1997**, *36*, 2752.

Chart 1



ligands was an intramolecular three-layered π stack.^{7b-d} Following this work a new four-armed ligand, 1,2,4,5-tetrakis(2-pyridylmethylsulfanylmethyl)benzene (**2tet**) was synthesized.^{6a} Its design was intended to allow for the formation of an intramolecular three-layered π -stacking motif and also to provide a possible route to two- or three-dimensional coordination polymers. However, in the only complex structurally characterized to date, $[\text{Cd}_2(\mathbf{2tet})(\text{NO}_3)_4]$, the ligand geometry led to ortho arms of the ligand chelating to the same Cd(II) ion, which resulted in the formation of discrete dinuclear complexes. To promote the formation of coordination polymers, by reducing the ability of the ligands to chelate, the isomeric 3- and 4-pyridyl substituted ligands 1,2,4,5-tetrakis(3-pyridylmethylsulfanylmethyl)benzene (**3tet**) and 1,2,4,5-tetrakis(4-pyridylmethylsulfanylmethyl)benzene (**4tet**) (Chart 1) have been synthesized. Reaction of these two ligands with a series of Ag(I) salts has led to the formation of three-dimensional coordination polymers. Those polymers incorporating **3tet** were seen to be isomorphous, while those that contained **4tet** also showed very similar arrangements of the ligands, despite the inherent flexibility. The persistent similar arrangement of the ligands and consequent structural similarities of the networks were unexpected given the flexibility of the ligand and the different anions and solvents incorporated in the networks. They appear to arise largely from the tendency of the S donors on the ortho arms to chelate to the same metal center thereby locking in, to a significant degree, the conformation of the ligand. Interestingly, the intramolecular three-layered π -stacking motif was not seen, although a related interligand motif was predominant. Topological analyses of the resulting network structures revealed them to be of either rare or

previously unknown topologies comprising both three- and six-connected nodes.

Experimental Section

General. The precursor 1,2,4,5-tetrakis(mercaptomethyl)benzene was prepared by the literature method.⁸ All ^1H , ^{13}C , and two-dimensional NMR spectra were measured with a 500 MHz Varian UNITYINOVA spectrometer, at 298 K, and referenced to the internal solvent signal. IR spectra were measured with a Perkin-Elmer Spectrum BX FT-IR System, with samples in KBr disks. ESMS was carried out on a Shimadzu LCMSQP800 α spectrometer with a mass range $m/z = 10\text{--}2000$. Samples were injected by direct infusion using a Rheodyne manual injector. The mobile phase flow rate was 0.2 mL min^{-1} and consisted of a 90% MeCN/10% H_2O solvent mixture. Elemental microanalyses were carried out at the Campbell Microanalytical Laboratory at the University of Otago. Samples were predried under vacuum to remove volatile solvent residues.

Caution. All perchlorate precursors and complexes should be treated as potentially explosive and be prepared in small amounts. No problems were encountered during the synthesis and characterization of the complexes prepared.

Ligands. Synthesis of 1,2,4,5-Tetrakis(3-pyridylmethylsulfanylmethyl)benzene (3tet). 1,2,4,5-Tetrakis(mercaptomethyl)benzene (6.0 g, 23 mmol) was added to a solution of 3-picolylchloride hydrochloride (15 g, 0.91 mol) in 350 mL of 30:70 (v/v) $\text{CH}_2\text{Cl}_2/\text{EtOH}$ containing NaOH (8 g). The mixture was stirred for 24 h. Solvent was removed in vacuo to leave a pale yellow oily solid. The residue was dissolved in 400 mL of CH_2Cl_2 and washed with water ($3 \times 400\text{ mL}$). The organic portion was dried (MgSO_4), and solvent was removed in vacuo to give a yellow-orange oily solid. The crude solid was purified by column chromatography (neutral alumina) eluting with CHCl_3 to give **3tet** as a pure pale brown solid. Yield 5.0 g (35%). Anal. Calcd for $\text{C}_{34}\text{H}_{34}\text{N}_4\text{S}_4 \cdot \text{H}_2\text{O}$: C, 63.31; H, 5.64; N, 8.69; S, 19.89%. Found: C, 62.97; H, 5.48; N, 8.31; S, 19.95%. $^1\text{H NMR}$ (CD_3CN): 8.46 (d, $^3J(\text{HH}) = 2.0\text{ Hz}$, 4H), 8.43 (dd, $^3J(\text{HH}) = 6.5\text{ Hz}$, $^4J(\text{HH}) = 1.5\text{ Hz}$, 4H), 7.64 (m, 4H), 7.27 (m, 4H), 7.01 (s, 2H), 3.64 (s, 8H), 3.63 (s, 8H) ppm. $^{13}\text{C NMR}$ (CD_3CN): 150.7, 149.0, 137.1, 135.9, 135.1, 133.4, 124.3, 34.1, 33.3 ppm. ESMS (MeCN): 628 m/z [**(3tet)**H] $^+$. Selected IR (KBr)/ cm^{-1} : 2913s, 1573s, 1477s, 1024s, 715s, 628s.

Synthesis of 1,2,4,5-Tetrakis(4-pyridylmethylsulfanylmethyl)benzene (4tet). 1,2,4,5-Tetrakis(mercaptomethyl)benzene (2.0 g, 7.62 mmol) was added to a solution of 4-picolylchloride hydrochloride (5.0 g, 30 mmol) in 600 mL of 30:70 (v/v) $\text{CH}_2\text{Cl}_2/\text{EtOH}$ containing NaOH (6 g). The mixture was stirred for 24 h. Solvent was removed in vacuo to leave a pale yellow residue. The residue was dissolved in 400 mL of CH_2Cl_2 , filtered, and washed with water ($3 \times 300\text{ mL}$). The organic portion was dried (MgSO_4), and solvent was removed in vacuo to give a brown solid. This was recrystallized from CH_2Cl_2 and hexane to give a tan solid. Yield 1.4 g (30%). Anal. Calcd for $\text{C}_{34}\text{H}_{34}\text{N}_4\text{S}_4$: C, 65.13; H, 5.48; N, 8.94; S, 20.46%. Found: C, 65.24; H, 5.70; N, 8.95; S, 20.32%. $^1\text{H NMR}$ (CDCl_3): 8.55 (dd, $^3J(\text{HH}) = 4.5\text{ Hz}$, $^4J(\text{HH}) = 1.5\text{ Hz}$, 8H), 7.20 (dd, $^3J(\text{HH}) = 4.5\text{ Hz}$, $^4J(\text{HH}) = 1.5\text{ Hz}$, 8H), 6.89 (s, 2H), 3.57 (s, 8H), 3.56 (s, 8H) ppm. $^{13}\text{C NMR}$ (CDCl_3): 150.1, 147.2, 134.9, 133.0, 123.9, 35.6, 32.8 ppm. ESMS (MeCN): 628 m/z [**(4tet)**H] $^+$. Selected IR (KBr)/ cm^{-1} : 3024m, 2918m, 1598s, 1413s, 991s, 567s.

Complexes. $\{[\text{Ag}_2(\mathbf{3tet})](\text{ClO}_4)_2\}_\infty$ (**1**). AgClO_4 (33 mg, 0.16 mmol) dissolved in 20 mL of degassed MeCN was added via cannula to **3tet** (50 mg, 80 μmol) dissolved in 20 mL of degassed

- (5) (a) Steel, P. J. *Acc. Chem. Res.* **2005**, *38*, 243–250. (b) McMorran, D. A.; Steel, P. J. *Inorg. Chem. Commun.* **2003**, *6*, 43–47. (c) Reger, D. L.; Semeniue, R. F.; Smith, M. D. *Inorg. Chem.* **2001**, *40*, 6545–6546. (d) Hartshorn, C. M.; Steel, P. J. *J. Chem. Soc., Dalton Trans.* **1998**, 3935–3940.
- (6) (a) Cordes, D. B.; Hanton, L. R. *Inorg. Chem. Commun.* **2005**, *8*, 967–970. (b) McMorran, D. A.; Hartshorn, C. M.; Steel, P. J. *Polyhedron* **2004**, *23*, 1055–1061. (c) McMorran, D. A.; Steel, P. J. *Chem. Commun.* **2002**, 2120–2121.
- (7) (a) Caradoc-Davies, P. L.; Gregory, D. H.; Hanton, L. R.; Turnbull, J. M. *J. Chem. Soc., Dalton Trans.* **2002**, 1574–1580. (b) Caradoc-Davies, P. L.; Hanton, L. R.; Henderson, W. *J. Chem. Soc., Dalton Trans.* **2001**, 2749–2755. (c) Caradoc-Davies, P. L.; Hanton, L. R. *Chem. Commun.* **2001**, 1098–1099. (d) Caradoc-Davies, P. L.; Hanton, L. R.; Lee, K. *Chem. Commun.* **2000**, 783–784. (e) Hanton, L. R.; Lee, K. *J. Chem. Soc., Dalton Trans* **2000**, 1161–1166.

- (8) Vinod, T.; Hart, H. *J. Org. Chem.* **1990**, *55*, 881–890.

Table 1. Crystallographic Data for Complexes

	1	2	3	4·2MeCN·2CHCl ₃	5·6MeCN	6·3H ₂ O
formula	C ₁₇ H ₁₇ AgClN ₂ O ₄ S ₂	C ₁₇ H ₁₇ AgF ₆ N ₂ PS ₂	C ₁₉ H ₁₇ AgF ₃ N ₂ O ₂ S ₂	C ₂₀ H ₂₁ AgCl ₄ N ₃ O ₄ S ₂	C ₂₃ H ₂₆ AgF ₆ N ₅ PS ₂	C ₁₈ H ₂₀ AgF ₃ N ₂ O _{4.5} S ₃
mol wt	520.77	566.29	534.34	681.19	689.45	597.41
cryst syst	orthorhombic	orthorhombic	orthorhombic	monoclinic	monoclinic	monoclinic
space group	<i>Pbca</i> (No. 61)	<i>Pbca</i> (No. 61)	<i>Pbca</i> (No. 61)	<i>P2₁/c</i> (No. 14)	<i>P2₁/c</i> (No. 14)	<i>C2/c</i> (No. 15)
<i>a</i> (Å)	12.550(5)	12.708(5)	12.887(5)	14.085(2)	14.044(3)	20.100(11)
<i>b</i> (Å)	13.508(5)	13.699(5)	14.284(5)	16.293(2)	16.321(3)	22.556(13)
<i>c</i> (Å)	22.083(5)	22.252(5)	21.617(5)	12.489(1)	13.627(3)	14.617(9)
β (deg)				112.425(1)	115.186(2)	123.276(10)
<i>U</i> (Å ³)	3744(2)	3874(2)	3979(2)	2649.3(5)	2826.5(9)	5540(5)
<i>Z</i>	8	8	8	4	4	8
<i>T</i> (K)	113(2)	118(2)	98(2)	163(2)	163(2)	113(2)
μ (mm ⁻¹)	1.470	1.402	1.269	1.354	0.980	0.999
no. of reflns collected	16 822	11 817	33 064	33 483	29 557	17 696
no. of unique	3689 (0.0652)	3917 (0.0997)	4077 (0.0344)	5453 (0.0254)	5777 (0.0309)	5419 (0.1224)
reflms (<i>R</i> _{int})						
<i>R</i> 1 indices [<i>I</i> > 2 σ (<i>I</i>)]	0.0616	0.0448	0.0274	0.0430	0.0411	0.0597
w <i>R</i> 2 (all data)	0.1963	0.0865	0.0689	0.1267	0.0939	0.1120
cryst size/mm ³	0.46 × 0.39 × 0.22	0.45 × 0.24 × 0.18	0.41 × 0.30 × 0.17	0.40 × 0.20 × 0.15	0.90 × 0.70 × 0.55	0.26 × 0.25 × 0.25
θ range	2.40–26.50	2.37–26.41	2.33–26.42	1.56–26.49	2.14–26.47	2.42–26.51
data/restraints/params	3689/20/291	3917/0/262	4077/0/290	5453/0/308	5777/0/346	5419/0/199

CH₂Cl₂ and stirred for 3 days. The brown solid which precipitated was filtered and dried in vacuo. Yield 60 mg (72%). Pale yellow X-ray quality crystals were grown from the slow diffusion of a CH₂Cl₂ solution of **3tet** layered with an MeCN solution of AgClO₄. Anal. Calcd for C₃₄H₃₄N₄O₈S₄Cl₂Ag₂: C, 39.20; H, 3.30; N, 5.38; S, 12.31; Cl, 6.81%. Found: C, 38.73; H, 3.30; N, 5.35; S, 12.01; Cl, 6.88%. Selected IR (KBr)/cm⁻¹: 2916m br (**3tet**), 1579m (**3tet**), 1479m (**3tet**), 1427m (**3tet**), 1088s br (ClO₄⁻), 1030m (**3tet**), 708m (**3tet**), 622m (**3tet**).

{[Ag₂(**3tet**)](PF₆)₂}_∞ (**2**). AgPF₆ (40 mg, 0.16 mmol) dissolved in 20 mL of degassed MeCN was added via cannula to **3tet** (50 mg, 80 μmol) dissolved in 20 mL of degassed CH₂Cl₂ and stirred 3 days. The brown solid which precipitated was filtered and dried in vacuo. Yield 37 mg (41%). Pale yellow X-ray quality crystals were grown from the slow diffusion of a CH₂Cl₂ solution of **3tet** layered with an MeCN solution of AgPF₆. Anal. Calcd for C₃₄H₃₄N₄F₁₂P₂S₄Ag₂: C, 36.05; H, 3.00; N, 4.95; S, 11.33%. Found: C, 35.84; H, 2.97; N, 4.80; S, 11.36%. Selected IR (KBr)/cm⁻¹: 2916m br (**3tet**), 1480w (**3tet**), 1427m (**3tet**), 840s br (PF₆⁻), 707m (**3tet**), 558m (**3tet**).

{[Ag₂(**3tet**)](CF₃CO₂)₂}_∞ (**3**). AgCF₃CO₂ (34 mg, 0.16 mmol) dissolved in 20 mL of degassed MeCN was added via cannula to **3tet** (50 mg, 80 μmol) dissolved in 20 mL of degassed CH₂Cl₂ and stirred overnight. The cream solid which precipitated was filtered and dried in vacuo. Yield 62 mg (72%). Pale yellow X-ray quality crystals were grown from the slow diffusion of a CH₂Cl₂ solution of **3tet** layered with an MeCN solution of AgCF₃CO₂. Anal. Calcd for C₃₈H₃₄N₄O₄F₆S₄Ag₂·2H₂O: C, 41.30; H, 3.47; N, 5.07; F, 10.32; S, 11.61%. Found: C, 41.22; H, 3.27; N, 5.03; F, 10.44; S, 11.77%. Selected IR (KBr)/cm⁻¹: 2925m br (**3tet**), 1685s (CF₃CO₂⁻), 1578m (**3tet**), 1478w (**3tet**), 1426m (**3tet**), 1199s (CF₃CO₂⁻), 1159m (CF₃CO₂⁻), 1117m br (CF₃CO₂⁻), 1029w (**3tet**), 716m (**3tet**), 635m (**3tet**).

{[Ag₂(**4tet**)](ClO₄)₂}_∞ (**4**). AgClO₄ (33 mg, 0.16 mmol) dissolved in 20 mL of degassed MeCN was added via cannula to **4tet** (50 mg, 80 μmol) dissolved in 20 mL of degassed CH₂Cl₂ and stirred overnight. The tan solid which precipitated was filtered and dried in vacuo. Yield 73 mg (88%). Pale yellow X-ray quality crystals of **4·2MeCN·2CHCl₃** were grown from the slow diffusion of a CHCl₃ solution of **4tet** layered with CH₂Cl₂ and an MeCN solution of AgClO₄. Anal. Calcd for C₃₄H₃₄N₄O₈S₄Cl₂Ag₂·2H₂O: C, 38.53; H, 3.43; N, 5.23; S, 12.11%. Found: C, 38.29; H, 3.20; N, 5.27;

S, 12.12%. Selected IR (KBr)/cm⁻¹: 2925m br (**4tet**), 1607s br (**4tet**), 1420m (**4tet**), 1081s br (ClO₄⁻), 1009w (**4tet**), 574m (**4tet**).

{[Ag₂(**4tet**)](PF₆)₂}_∞ (**5**). AgPF₆ (40 mg, 0.16 mmol) dissolved in 20 mL of degassed MeCN was added via cannula to **4tet** (50 mg, 80 μmol) dissolved in 20 mL of degassed CH₂Cl₂ and stirred for 3 days. The tan solid which precipitated was filtered and dried in vacuo. Yield 66 mg (73%). Yellow X-ray quality crystals of **5·6MeCN** were grown from the slow diffusion of a CHCl₃ solution of **4tet** layered with CH₂Cl₂ and an MeCN solution of AgPF₆. Anal. Calcd for C₃₄H₃₄N₄F₁₂P₂S₄Ag₂: C, 36.05; H, 3.03; N, 4.95; S, 11.33%. Found: C, 36.42; H, 2.99; N, 4.87; S, 11.53%. Selected IR (KBr)/cm⁻¹: 2927m br (**4tet**), 1610s (**4tet**), 1423m (**4tet**), 840s br (PF₆⁻), 556m (**4tet**).

{[Ag₂(**4tet**)](CF₃SO₃)₂}_∞ (**6**). AgCF₃SO₃ (41 mg, 0.16 mmol) dissolved in 20 mL of degassed MeCN was added via cannula to **4tet** (50 mg, 80 μmol) dissolved in 20 mL of degassed CH₂Cl₂ and stirred overnight. The tan solid which precipitated was filtered and dried in vacuo. Yield 66 mg (72%). Colorless X-ray quality crystals of **6·3H₂O** were grown from the slow diffusion of a CH₂-Cl₂ solution of **4tet** layered with an MeCN solution of AgCF₃SO₃. Anal. Calcd for C₃₄H₃₄N₄O₆F₆S₆Ag₂·3H₂O: C, 36.18; H, 3.38; N, 4.69; S, 16.10%. Found: C, 35.90; H, 3.07; N, 4.25; S, 16.06%. Selected IR (KBr)/cm⁻¹: 2923m br (**4tet**), 1609s (**4tet**), 1420m (**4tet**), 1262m br (CF₃SO₃⁻), 1174m br (CF₃SO₃⁻), 1031m (CF₃SO₃⁻), 572m (**4tet**).

X-ray Crystallography. Diffraction data were collected at the University of Canterbury, New Zealand, on a Bruker SMART CCD diffractometer, with graphite-monochromated Mo K α (λ = 0.71073 Å) radiation. Intensities were corrected for Lorentz polarization effects,⁹ and a multiscan absorption correction¹⁰ was applied. The structures were solved by direct methods (SHELXS¹¹ or SIR-97¹²) and refined on *F*² using all data by full-matrix least-squares procedures (SHELXL 97).¹³ All calculations were performed using

(9) SAINT, Area Detector Control and Integration Software version 4; Siemens Analytical X-ray Systems, Inc.: Madison, WI, 1996.

(10) Sheldrick, G. M. SADABS, Program for Absorption Correction; University of Göttingen: Göttingen, Germany, 1996.

(11) Sheldrick, G. M. Acta Crystallogr., Sect. A 1990, 46, 467–473.

(12) Altomare, A.; Burla, M. C.; Camalli, M.; Cascarano, G. L.; Giacovazzo, C.; Guagliardi, A.; Moliterni, A. G. G.; Polidori, G.; Spagna, R. J. Appl. Crystallogr. 1999, 32, 115–119.

(13) Sheldrick, G. M. SHELXL 97; University of Göttingen: Göttingen, Germany, 1997.

the WinGX interface.¹⁴ Crystallographic data for the six structures are listed in Table 1. Minor disorder was observed in the anions in **1** and **3**. In **1** the ClO_4^- anions were disordered by translation over two sites, having site occupancy factors of 0.47 and 0.53. In **3** the CF_3 groups of the CF_3CO_2^- anions were disordered about a 3-fold axis over two sites, with three of the fluorine atoms having a site occupancy factor of 0.79 and the other three fluorine atoms having a site occupancy factor of 0.21

Results and Discussion

Ligand Synthesis. Both isomeric ligands **3tet** and **4tet** were prepared by the thioether base coupling of 1,2,4,5-tetrakis(mercaptomethyl)benzene and the appropriate picolylchloride hydrochloride salt in a 1:4 ratio. The precursor 1,2,4,5-tetrakis(mercaptomethyl)benzene was prepared in excellent yield from 1,2,4,5-tetrakis(bromomethyl)benzene according to the literature procedure.⁸ Purification of **3tet** was accomplished by column chromatography over neutral alumina, eluting with CHCl_3 to give a pale brown solid, while **4tet** was purified by recrystallization from CH_2Cl_2 /hexane to give a tan solid.

Syntheses and Structures of 1, 2, and 3. The 2:1 molar reactions of AgClO_4 , AgPF_6 , or AgCF_3CO_2 in degassed MeCN and **3tet** in degassed CH_2Cl_2 were stirred, resulting in precipitates of **1–3** which gave microanalytical data consistent in all three cases with 2:1 metal-to-ligand ratios. The complexes **1–3** were insoluble in most common organic solvents. The IR spectrum of **1** showed only one peak in the ClO_4^- stretching region, a strong and broad feature at 1088 cm^{-1} , consistent with the ClO_4^- anion not coordinating to the Ag(I).¹⁵ The IR spectrum of **2** showed only one peak in the PF_6^- stretching region, a strong and broad feature at 840 cm^{-1} , consistent with the PF_6^- anion not interacting strongly with the Ag(I).¹⁶ The IR spectrum of **3** showed four peaks at correct positions to be CF_3CO_2^- , a strong peak at 1685 cm^{-1} and a strong and very broad feature made up of three peaks at $1199\text{--}1117\text{ cm}^{-1}$. These peaks suggested that the CF_3CO_2^- was not coordinated,¹⁶ although the splitting of the $-\text{CF}_3$ stretches indicated that interactions might be occurring to distort the $-\text{CF}_3$ group. In all complexes additional peaks indicative of the presence of the ligand were seen (vide supra).

X-ray structural analyses revealed that all three complexes formed isomorphous three-dimensional network structures which crystallized in the orthorhombic space group *Pbca*. The network structures formed showed a complex and uncommon topology. In all cases the asymmetric unit consisted of one Ag(I) cation, half a **3tet** ligand, and one counteranion. The central benzene ring of the ligand was on a center of symmetry. Each ligand was bonded to six four-coordinate Ag(I) ions, two via chelation by S donors on ortho pyridine arms and the other four via coordination by N_{py} donors (Figure 1). The Ag(I) ions in turn coordinated to two

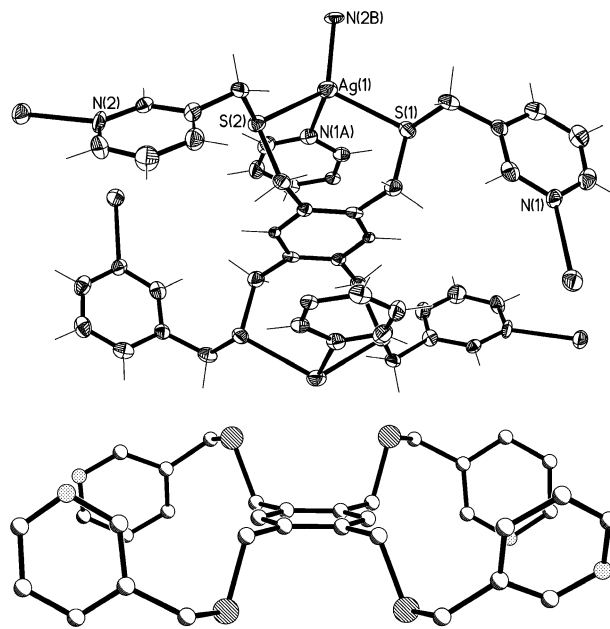


Figure 1. (top) View of the coordination sphere of complex **2** (crystallographic numbering) also showing the interligand three-layered π stack, with PF_6^- anions omitted for clarity. Thermal ellipsoids drawn at the 50% probability level. Selected bond lengths (\AA) and angles (deg): N(1B)–Ag(1) 2.475(5), N(2A)–Ag(1) 2.281(4), S(1)–Ag(1) 2.5491(15), S(2)–Ag(1) 2.5288(16); N(2A)–Ag(1)–N(1B) 99.01(16), N(2A)–Ag(1)–S(2) 128.92(11), N(1B)–Ag(1)–S(2) 93.93(11), N(2A)–Ag(1)–S(1) 115.22(12), N(1B)–Ag(1)–S(1) 98.82(11), S(2)–Ag(1)–S(1) 111.13(5). (Symmetry codes: A, $x + 1/2, -y + 1/2, -z$; B, $-x, y + 1/2, -z + 1/2$). (bottom) A view showing the planarity of **3tet** in complexes **1–3** and the relative orientations of pyridine rings. Anions, Ag(I) cations, and hydrogen atoms omitted.

other adjacent ligands, meaning that each ligand was linked by Ag coordination to 12 adjacent ligands. Thus, each Ag(I) ion was bound in a tetrahedral fashion by $\text{N}_{\text{py}}\text{N}_{\text{py}}'$ donors from two ligands and $\text{S}''\text{S}''$ donors from a third (Figure 1). The N_{py} – and S–Ag bond distances fell close to the middle of the range ($2.09\text{--}2.82\text{ \AA}$ from 1080 bond distances in 440 complexes and $2.32\text{--}3.32\text{ \AA}$ from 556 bond distances in 235 complexes, respectively) as determined by searches of the CSD (version 5.26) for four-coordinate complexes containing Ag– N_{py} and thioether Ag–S bond distances.¹⁷ The bridging nature of the Ag(I) ions led to the formation of the three-dimensional coordination polymers.

The ligands were arranged with all four pyridine arms in a stretched-out fashion (Figure 1). Each pair of ortho pyridine arms had a similar conformation, the S atoms binding to the Ag(I) ions to give seven-membered metallamacrocyclic rings. One ortho pair of arms was arranged with its S atoms above the plane of the central benzene ring, the other below; however, the ends of the arms were folded back, such that the centroids of all four pyridine rings were in the plane of the central ring (mean deviations from the plane ranged from 0.005 to 0.062 \AA). However, the direction in which the pyridine ring pointed, relative to the central ring, differed between ortho pyridine arms (Figure 1). One pyridine donor pointed away from one face of the central ring and was

(14) Farrugia, L. J. *J. Appl. Crystallogr.* **1999**, *32*, 837–838.

(15) Nakamoto, K. *Infrared and Raman Spectra of Inorganic and Coordination Compounds, Part B*, 5th ed.; Wiley–Interscience: New York, 1997.

(16) Socrates, G. *Infrared and Raman Characteristic Group Frequencies*; John Wiley and Sons Ltd.: Chichester, 2001.

(17) Allen, F. H.; Davies, J. E.; Galloy, J. J.; Johnson, O.; Kennard, O.; Macrae, C. F.; Mitchell, E. M.; Mitchell, G. F.; Smith, J. M.; Watson, D. G. *J. Chem. Inf. Comput. Sci.* **1991**, *31*, 187–204.

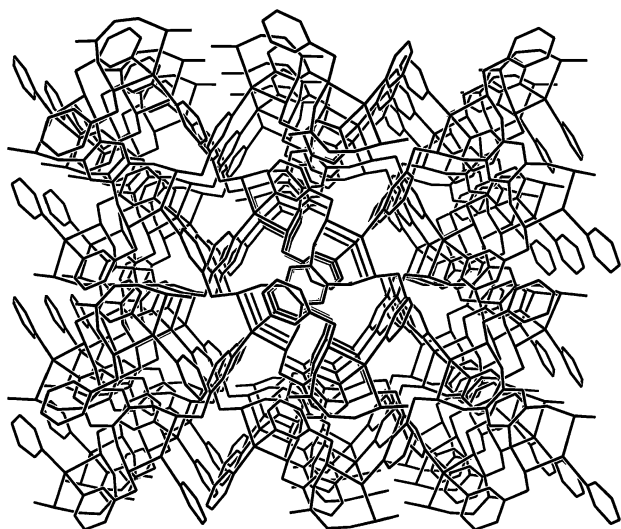


Figure 2. View down the crystallographic a axis of the three-dimensional cationic framework of complex **2**, with hydrogen atoms and PF_6^- anions omitted for clarity.

approximately orthogonal to the plane of that ring, whereas the other pointed away from the opposite face of the central ring but was closer to parallel with the plane of the central ring. This meant that while meta pyridine rings can be viewed so that they eclipse each other, the N_{py} atoms point to the same side of the plane of the central ring, but at different angles. Both pyridine rings were close to orthogonal to the central ring; in **1** one ring was inclined at 85.4° , the other at 67.5° , in **2** one ring was at 88.0° , the other at 66.6° , and in **3** one ring was at 91.2° , the other at 70.6° . Relative to each other, the pyridine rings were inclined at 32.4° in **1**, 32.1° in **2**, and 30.5° in **3**. Overall, the **3tet** molecules in all three complexes were arranged in virtually identical fashions, with most of the differences due to slight changes in folding at $-\text{CH}_2-$ groups or small rotations of $\text{C}-\text{C}$ bonds. These changes were probably caused by the overall framework having to accommodate anions ranging in size from the small BF_4^- to larger PF_6^- and CF_3CO_2^- .

The resulting three-dimensional arrays assembled themselves so that, in all three structures, two symmetry-related pyridine rings from different ligands were able to form a strongly interacting interligand, three-layered π stack by interacting with the central ring of a third ligand (centroid-to-centroid distances 3.59 [**1**], 3.63 [**2**], and 3.70 Å [**3**]) (Figures 1 and 2). The rings in the π stacks were very close to parallel, with angles between them ranging from 3.9° to 5.2° . This interligand π -stacked arrangement was different than the way related ligands had formed three-layer stacks in previously reported work, as there they form intraligand stacks.^{7b-d} There have been a small number of other reported examples of interligand three-layer stacks, although the ligand systems they occur in are very different from the one being considered here.¹⁸ The pyridine rings that were involved in this three-layered π stack in **1–3** were also involved in edge-to-face $\text{C}-\text{H}\cdots\pi$ interactions with pyridine rings on other adjacent ligands, with $\text{C}-\text{H}\cdots$ centroid and corresponding $\text{C}\cdots$ centroid distances of 2.81 and 3.55 (**1**), 2.92 and 3.66 (**2**), and 3.17 and 3.93 Å (**3**), respectively.

These distances were close to the conventional van der Waals limit, but $\text{CH}\cdots\pi$ interactions have been suggested to be effective at distances beyond this value.^{19,20} In all three complexes the anion had a variety of weak interactions with either or both alkyl and aryl hydrogens. The disordered ClO_4^- anions (**1**) had $\text{O}_3\text{Cl}-\text{O}\cdots\text{H}-\text{C}$ separations in the range 2.25 – 2.56 Å and corresponding $\text{O}\cdots\text{C}$ separations of 3.19 – 3.51 Å. The PF_6^- anions (**2**) had $\text{F}_5\text{P}-\text{F}\cdots\text{H}-\text{C}$ separations in the range 2.34 – 2.47 Å and corresponding $\text{F}\cdots\text{C}$ separations of 3.21 – 3.31 Å. The CF_3CO_2^- anions (**3**) had $\text{CF}_3-\text{CO}-\text{O}\cdots\text{H}-\text{C}$ separations in the range 2.29 – 2.50 Å and corresponding $\text{O}\cdots\text{C}$ separations of 3.21 – 3.37 Å. This confirmed the IR data, which in all cases showed no obvious changes of symmetry and indicated that the anions did not coordinate to the $\text{Ag}(\text{I})$ ion. However, the peak broadening or minor splitting seen in the relevant areas of the IR spectra could be due to solid-state effects such as the weak interactions noted here.

The three-dimensional arrays were analyzed using PLATON,²¹ and no solvent-accessible volume was found (Figure 2). The packing index for each of the frameworks (anion included) was calculated. In the cases of **1** and **3** the packing index was estimated by averaging the values of packing indices output by PLATON for the structures of each of the two disordered solvent components, weighted for their occupancy. The packing index for **2** was calculated as 0.75 , which showed good agreement with the estimated values for **1** and **3** (0.74 and 0.73 , respectively). The packing indices for the cationic frameworks with anion removed were also, as expected, very similar and ranged from 0.60 to 0.63 .

Syntheses and Structures of 4·2MeCN·2CHCl₃ and 5·6MeCN. The 2:1 molar reactions of AgClO_4 (**4**) or AgPF_6 (**5**) in degassed MeCN and **4tet** in degassed CH_2Cl_2 were stirred, resulting in precipitates which gave microanalytical data consistent in both cases with 2:1 metal-to-ligand ratios. The complexes were insoluble in most common organic solvents. The IR spectrum of **4** showed only one peak in the ClO_4^- stretching region, a strong and broad feature at 1088 cm^{-1} , consistent with the ClO_4^- anion not coordinating to the $\text{Ag}(\text{I})$ ion.¹⁵ The IR spectrum of **5** showed only one peak in the PF_6^- stretching region, a strong and broad feature at 840 cm^{-1} , consistent with the PF_6^- anion not coordinating to the $\text{Ag}(\text{I})$ ion.¹⁶ Also present in both complexes were peaks indicative of the ligand (vide supra).

X-ray structural analysis revealed that both complexes formed porous isotopological three-dimensional network structures of complex and uncommon topology, crystallizing

- (18) (a) Xu, F.-B.; Xu, H.; Leng, X.-B.; Song, H.-B.; Li, Q.-S.; Zou, R.-Y.; Zhang, Z.-Z. *Acta Crystallogr.* **2003**, *E59*, m1044–m1045. (b) Chanda, N.; Laye, R. H.; Chakraborty, S.; Paul, R. L.; Jeffery, J. C.; Ward, M. D.; Lahiri, G. K. *J. Chem. Soc., Dalton Trans.* **2002**, 3496–3504. (c) Paul, R. L.; Bell, Z. R.; Jeffery, J. C.; McCleverty, J. A.; Ward, M. D. *Proc. Natl. Acad. Sci. U.S.A.* **2002**, *99*, 4883–4888. (d) Bell, Z. R.; Jeffery, J. C.; McCleverty, J. A.; Ward, M. D. *Angew. Chem., Int. Ed.* **2002**, *41*, 2515–2518.
- (19) (a) Nishio, M. *CrystEngComm* **2004**, *6*, 130–158. (b) Umezawa, Y.; Tsuboyama, S.; Honda, K.; Uzawa, J.; Nishio, M. *Bull. Chem. Soc. Jpn.* **1998**, *71*, 1207–1213. (c) Nishio, M.; Umezawa, Y.; Hirota, M.; Takeuchi, Y. *Tetrahedron* **1995**, *51*, 8665–8701.
- (20) Dance, I. *New J. Chem.* **2003**, *27*, 22–27.
- (21) PLATON: Spek, A. L. *J. Appl. Cryst.* **2003**, *36*, 7–13.

in the monoclinic space group $P2_1/c$. Despite the similarity of the dimensions of the unit cells of the complexes, they were determined not to be isomorphous. In both cases the asymmetric unit consisted of one Ag(I) cation, half a **4tet** ligand, one counteranion and solvent molecules. In **4**·**2MeCN**·**2CHCl₃** the solvent present was one molecule of CHCl₃ and one molecule of MeCN, whereas in **5**·**6MeCN** it was three molecules of MeCN. The central benzene ring of the ligand was on a center of symmetry. Each ligand was bonded to six, four-coordinate Ag(I) ions, two via chelation by S donors on ortho pyridine arms and the other four via coordination by N_{py} donors (Figure 3). The Ag(I) ions in turn coordinated to two further ligands, meaning that each ligand was linked by Ag coordination to 12 adjacent ligands. The bridging nature of the Ag(I) ions led to the formation of the three-dimensional coordination polymer. Each Ag(I) ion was bound in a tetrahedral fashion by N_{py}N_{py'} donors from two ligands and S''S' donors from a third (Figure 3). The N_{py}– and S–Ag bond distances fell close to the middle of the range of N_{py}–Ag and thioether S–Ag bond lengths (2.09–2.82 and 2.32–3.32 Å, respectively) as determined by a search of the CSD.¹⁷

The ligands were arranged with one pair of symmetry-related para pyridine arms in a stretched-out fashion, somewhat similar to that seen in complexes **1**–**3**. The centroids of these two pyridine rings lay in the plane of the central ring (mean deviation from plane 0.077 Å for **4**·**2MeCN**·**2CHCl₃**, 0.006 Å for **5**·**6MeCN**). The other pair of para pyridine arms had its pyridine rings folded away from the central ring, rather than toward it, leading to a more stepped conformation for one para pair of arms than the other (Figure 3). Each ortho pair of pyridine arms was arranged with its S atoms either above the plane of the central benzene ring or below, with the S atoms able to bind to the Ag(I) ion to form seven-membered metallamacrocyclic rings. The direction in which the pyridine ring pointed, relative to the central ring, differed between ortho pyridine arms. One pyridine donor pointed away from one face of the central ring and was approximately orthogonal to the plane of that ring, whereas the other pointed away from the opposite face of the central ring but was closer to parallel with the plane of the central ring (Figure 3). The planes of the pyridine rings were close to orthogonal to the central ring. In **4**·**2MeCN**·**2CHCl₃** one ring was inclined at 68.5°, the other at 108.2°, and in **5**·**6MeCN** one ring was at 51.0°, the other at 83.6°, all relative to the central ring. Relative to each other, the pyridine rings were closer to orthogonal than in the **3tet** structures, the angle between the rings being 80.1° (**4**·**2MeCN**·**2CHCl₃**) and 57.5° (**5**·**6MeCN**). Overall, the **4tet** molecules in both complexes were arranged in similar fashions, with most differences due to slight changes in folding at –CH₂– groups or small rotations of bonds. These changes were probably caused by the overall framework having to accommodate different-sized ClO₄[–] and PF₆[–] anions.

The three-dimensional arrays formed such that in both complexes, two symmetry-related pyridine rings from different ligands were able to form an interligand, three-layered

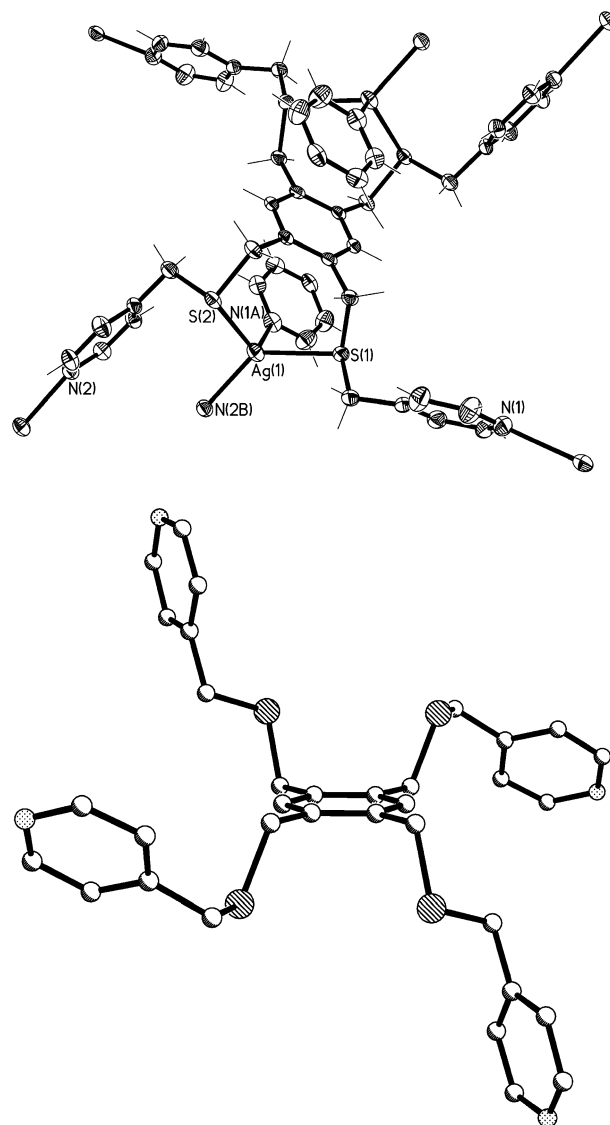


Figure 3. (top) View of the coordination sphere of complex **5**·**6MeCN** (crystallographic numbering) also showing the interligand three-layered π stack, with PF₆[–] anions and MeCN solvent molecules omitted for clarity. Thermal ellipsoids drawn at the 50% probability level. Selected bond lengths (Å) and angles (deg): N(1A)–Ag(1) 2.393(3), N(2B)–Ag(1) 2.280(3), S(1)–Ag(1) 2.559(9), S(2)–Ag(1) 2.576(10); N(2B)–Ag(1)–N(1A) 100.69(10), N(2B)–Ag(1)–S(1) 133.22(7), N(1A)–Ag(1)–S(1) 94.30(7), N(2B)–Ag(1)–S(2) 105.89(7), N(1A)–Ag(1)–S(2) 119.87(8), S(1)–Ag(1)–S(2) 104.19(3). (Symmetry codes: A, $-x, y + 1/2, -z + 1/2$; B, $-x, -y, -z + 1$). (bottom) A view showing the arrangement of **4tet** in complexes **4** and **5** and the relative orientations of pyridine rings. Anions, Ag(I) cations, and hydrogen atoms omitted.

π stack by interacting with the central ring of a third ligand [centroid-to-centroid distances 3.72 (**4**·**2MeCN**·**2CHCl₃**) and 3.95 Å (**5**·**6MeCN**)] (Figures 3 and 4). This π stack was very similar to the ones seen in complexes **1**–**3**, although the distances between centroids were longer for the **4tet** complexes. The rings in the stacks were close to parallel, with angles between them of only 4.9° for **4**·**2MeCN**·**2CHCl₃** and 14.5° for **5**·**6MeCN**. The other pyridine rings also took part in different two-layered π -stacking interactions with symmetry-related pyridine rings [centroid-to-centroid distance 3.80 (**4**·**2MeCN**·**2CHCl₃**) and 3.68 Å (**5**·**6MeCN**)], and were strictly parallel due to their symmetry. In contrast to the complexes of **3tet**, there were no interligand C–H \cdots π

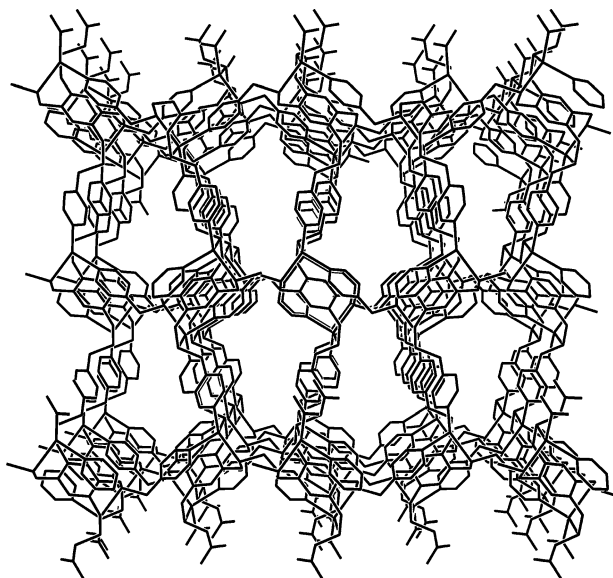


Figure 4. View down the crystallographic c axis of the three-dimensional cationic framework of complex **5** with PF_6^- anions and hydrogen atoms omitted for clarity.

interactions in these structures. The solvent molecules in the two complexes were held in place by a number of interactions. In **4**·**2MeCN**·**2CHCl₃** the MeCN solvent molecules were held in place in the framework by one direct set of interactions. They formed weak C—H··· π (pyridine) interactions with the framework at a distance of 3.05 Å. This distance is close to the van der Waals limit, but CH— π interactions have been suggested to be effective at distances beyond this value.^{19,20} The MeCN molecules also formed a C—Cl···H—C interaction with the solvent CHCl_3 molecules at a distance of 2.69 Å with corresponding Cl···C separation of 3.61 Å. The CHCl_3 molecules were only very loosely held in place, as they interacted only with the MeCN molecules and the ClO_4^- anions ($\text{O}_3\text{Cl—O}\cdots\text{H—C}$ separation 2.24 Å, corresponding $\text{O}\cdots\text{C}$ separation of 3.21 Å). In **5**·**6MeCN** the solvent MeCN molecules in the structure were held in their places in the framework by very weak N···H—C interactions between MeCN N atoms and both alkyl and aryl C—H. Distances ranged from 2.54 to 2.92 Å, with C···C separations of 3.24–3.88 Å. In both complexes the anion had a variety of weak interactions with either or both alkyl and aryl hydrogens. The ClO_4^- anions in **4**·**2MeCN**·**2CHCl₃** had an $\text{O}_3\text{Cl—O}\cdots\text{H—C}$ separation of 2.47 Å and a corresponding $\text{O}\cdots\text{C}$ separation of 3.40 Å, while the PF_6^- anions in **5**·**6MeCN** had $\text{F}_5\text{P—F}\cdots\text{H—C}$ separations in the range 2.38–2.55 Å and corresponding $\text{F}\cdots\text{C}$ separations of 3.20–3.39 Å. This confirmed the assumption, made on the basis of the IR data, that the anions did not coordinate to the Ag(I) ion. However, the peak broadening or minor splitting seen in the relevant peaks of the IR spectra could be due to the weak interactions noted here.

When the frameworks of the two complexes were compared it was clear that they were very similar in structure but were not considered to be isomorphous. The frameworks had formed in such a manner that they were skewed with respect to each other, so that the [1 0 1] diagonal axis in **4**·**2MeCN**·**2CHCl₃** was the a axis in **5**·**6MeCN** (Figure 5).

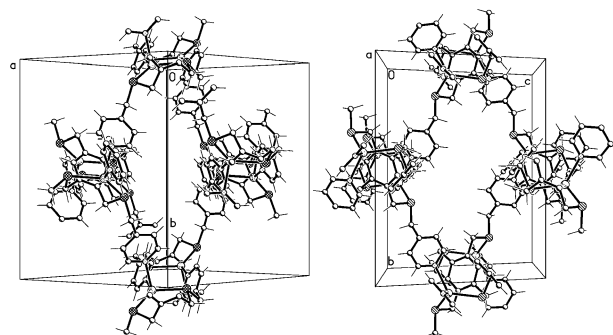


Figure 5. Views of the three-dimensional structures of **4** and **5** showing the skew of the frameworks relative to the unit cells. Anions omitted for clarity. (left) **4** viewed down the crystallographic [1 0 1] axis. (right) **5** viewed down the crystallographic a axis.

Both frameworks generated a number of different-sized pores. They had large ($11 \times 6 \text{ \AA}^2$) octagonal pores running along the c axis (Figure 4) and further large ($13 \times 6 \text{ \AA}^2$) tetragonal pores running along the [1 0 1] diagonal axis (**4**·**2MeCN**·**2CHCl₃**) or the a axis (**5**·**6MeCN**) (Figure 4). There were also several smaller pores in the framework, averaging about $5 \times 5 \text{ \AA}^2$, running along other diagonal and primary axes. The combined volume of the pores in the cationic frameworks was 45.6% (**4**·**2MeCN**·**2CHCl₃**) or 50.5% (**5**·**6MeCN**) of the unit cell volume, with packing indices of 0.45 and 0.42, respectively. All these values were calculated using PLATON and did not include anion or solvent.²¹ However, when the structure as a whole was considered, the pores were filled with solvent and anion, leading to the framework having no residual solvent-accessible volume (packing index 0.70 in both cases).²¹

Synthesis and Structure of 6·**3H₂O**. The 2:1 molar reaction of AgCF_3SO_3 and **4tet** in degassed MeCN and CH_2Cl_2 was stirred, resulting in a precipitate which gave microanalytical data consistent with a 2:1 metal-to-ligand ratio. The complex was insoluble in most common organic solvents. The IR spectrum showed three peaks for CF_3SO_3^- , all of moderate intensity: a broad feature at 1262 cm^{-1} , another broad feature at 1174 cm^{-1} , and a peak at 1031 cm^{-1} . These peaks were consistent with the CF_3SO_3^- anion not coordinating to the Ag(I) and not being structurally distorted by the interaction in the complex.¹⁶ Also present were peaks indicative of the ligand (vide supra).

X-ray structural analysis of this complex revealed a three-dimensional, porous network structure, crystallizing in the monoclinic space group $C2/c$. The asymmetric unit consisted of one Ag(I) cation, half a **4tet** ligand, one CF_3SO_3^- anion, and highly diffuse solvent molecules. The CF_3SO_3^- counterion was disordered and in addition could not be completely located. All attempts to model satisfactorily this disorder were unsuccessful. Therefore, the disordered anion and solvent residues were removed from the atom list for refinement, and the PLATON SQUEEZE²¹ procedure was applied. The residual electron density in the asymmetric unit was assigned to a whole CF_3SO_3^- counteranion and one and a half molecules of H_2O solvent. The central benzene ring of the ligand was on a center of symmetry. Each ligand was bonded to six four-coordinate Ag(I) ions, two via chelation by S donors on ortho pyridine arms the other four via coordination

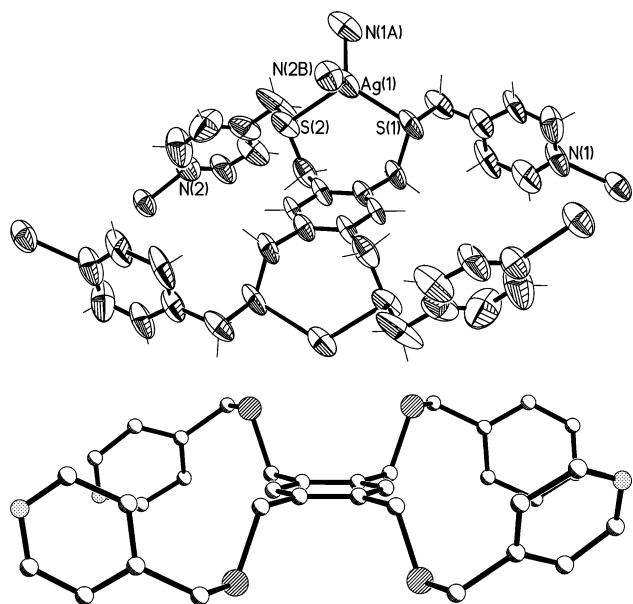


Figure 6. (top) View of the coordination environment of complex **6** (crystallographic numbering) with the thermal ellipsoids drawn at the 50% probability level. Selected bond lengths (Å) and angles (deg): N(1A)–Ag(1) 2.218(7), N(2B)–Ag(1) 2.305(6), S(1)–Ag(1) 2.484(3), S(2)–Ag(1) 2.555(2); N(1A)–Ag(1)–N(2B) 115.0(3), N(1A)–Ag(1)–S(1) 118.52(19), N(2B)–Ag(1)–S(1) 102.70(17), N(1A)–Ag(1)–S(2) 104.88(17), N(2B)–Ag(1)–S(2) 101.81(18), S(1)–Ag(1)–S(2) 112.93(7). (Symmetry codes: A, $x, -y, z - 1/2$; B, $x + 1/2, -y + 1/2, z - 1/2$). (bottom) A view showing the planarity of **4tet** in complex **6** and the relative orientations of pyridine rings. Anions, Ag(I) cations, and hydrogen atoms omitted.

by N_{py} donors (Figure 6). The Ag(I) ions in turn coordinated to two adjacent ligands, meaning that each ligand was linked by Ag coordination to 12 adjacent ligands. The bridging nature of the Ag(I) ions led to the formation of the three-dimensional coordination polymer. Each Ag(I) ion was bound in a tetrahedral fashion by $N_{py}N_{py}'$ donors from two ligands and $S''S''$ donors from a third (Figure 6). The N_{py} – and S –Ag bond distances fell close to the middle of the range of N_{py} –Ag and thioether S –Ag bond lengths (2.09–2.82 and 2.32–3.32 Å, respectively) as determined by a search of the CSD.¹⁷

The ligands were arranged with all four pyridine arms in a stretched-out fashion (Figure 6), very similar to that seen in the complexes of **3tet**. Each pair of ortho pyridine arms had a similar conformation, with the S atoms binding to the Ag(I) ions to give seven-membered metallamacrocyclic rings. One ortho pair of arms was arranged with its S atoms above the plane of the central benzene ring, the other below; however, the ends of the arms were folded back, so that the centroids of all four pyridine rings were in the plane of the central ring (mean deviation from plane 0.032 Å). Both pyridine donors of ortho pyridine arms pointed away from the same face of the central ring and did so at similar angles to the plane of the ring. This meant that while meta pyridine rings can be viewed so that they eclipse each other, the N_{py} atoms point to the opposite sides of the plane of the central ring (Figure 6). This differed from the **3tet** complexes, where meta rings pointed to the same side of the plane of the central ring, but at different angles. Both pyridine rings were close to orthogonal to the central ring, with one ring inclined at 84.4° and the other at 61.6°, both relative to the central ring.

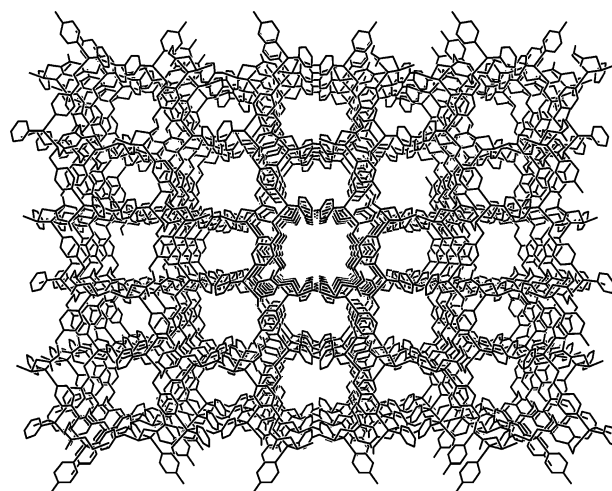


Figure 7. View down the crystallographic c -axis of the large pores formed in the three-dimensional cationic framework of **6**, with hydrogen atoms omitted for clarity.

Relative to each other, the pyridine rings were approximately coplanar, with an angle between planes of 33.2°.

The three-dimensional array was formed so that two symmetry-related pyridine rings from different ligands were able to form an edge-to-face $C-H\cdots\pi$ interaction with the central ring of a third ligand with a $C-H\cdots$ centroid distance of 2.98 Å and corresponding $C\cdots$ centroid distances of 3.74 Å. This distance was close to the conventional van der Waals limit, but $CH\cdots\pi$ interactions have been suggested to be effective at distances beyond this value.^{19,20} The way the ligands related to each other in **6·3H₂O** was very different to the way they related in other complexes (**4·2MeCN·2CHCl₃** and **5·6MeCN**) and how **3tet** had behaved in complexes **1–3**, as all the ligands in these cases formed three-layered π stacks. Anion and solvent interactions could not be considered for this structure because of the application of the SQUEEZE procedure.²¹

The framework generated a number of different sized pores. Large (9×9 Å²) tetragonal pores running along the c axis (Figure 7) and slightly smaller (9×5 Å²) hexagonal pores running along the [1 0 1] and the [1 1 0] diagonal axes. There were also a number of smaller pores in the framework, averaging about 5×5 Å², running along the other diagonal and primary axes. The combined volume of the pores in the cationic frameworks was 48.3% of the unit cell volume, with a packing index of 0.42. These values were calculated using PLATON²¹ from the SQUEEZED data. However, early attempts at modeling the disordered anions and solvent molecules showed them to be filling these pores.

Topological Analysis. Topological analyses were conducted using OLEX²² on all six complexes. In all cases non-coordinated solvent or anions were not considered to contribute to the topological network. Complexes **1–3** were found to be isomorphous and will be considered together, as will the isotopological complexes **4** and **5**. All three topological analyses showed the three topologies to be somewhat similar, as each comprised a six-connected ligand

(22) OLEX: Dolomanov, O. V.; Blake, A. J.; Champness, N. R.; Schröder, M. *J. Appl. Crystallogr.* **2003**, *36*, 1283–1284.

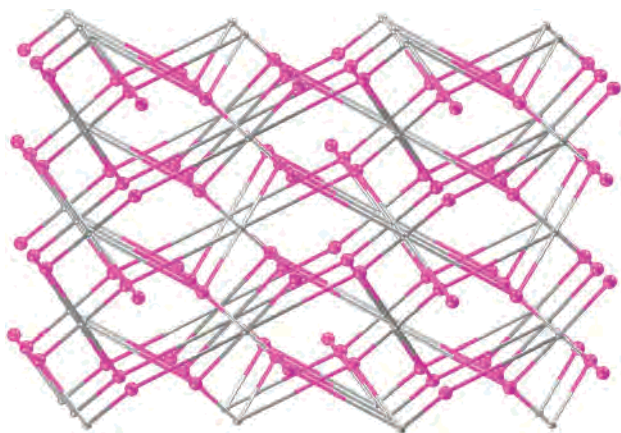


Figure 8. View along the *a* axis of the three-dimensional pyrite-like topological net formed by **3** (Ag nodes, pink; ligand nodes, gray).

node and two three-connected Ag nodes. Coordination polymers built around six-connected nodes have previously been found infrequently. The majority of these have metal ions or clusters as the six-connected nodes, with only four containing six-connected, ligand-based nodes.^{4c,d,23}

The topological network for **1–3** comprised two different nodes, one ligand-based and one Ag-based, indicating that topologically all ligands were the same, as were all Ag centers. The ligand node occurred where the centroid of the central ring would occur and had links to six Ag nodes, one link for each pyridine arm, and another for each pair of chelated S atoms, resulting in the ligand nodes having short topological terms of $6^{12,8^3}$. The Ag nodes in turn were three connected with short topological terms of 6^3 (Figure 8). Of these two nodes, the 6^3 node is not uncommon²⁴ and has been recognized to form the (6, 3) “honeycomb” net when it is the only node present.²⁵ Although, this topological functionality is more commonly seen in a two-dimensional rather than a three-dimensional array, there are some examples of 6^3 nodes as part of a more topologically complex network.²⁶ Often “honeycomb-like” two-dimensional sheets remain evident in the net; however, some of the nodes adopt higher coordination in order to link sheets together into a three-dimensional array. However, in **1–3** the six-membered circuits extending from the 6^3 nodes are three-, rather than two-dimensional (Figure 8). This particular combination of three- and six-connected nodes is also found in the topologi-

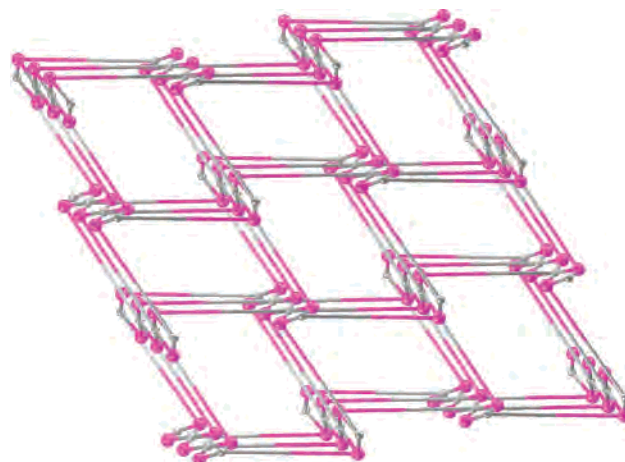


Figure 9. View along the *a* axis of the three-dimensional rutile-like topological net formed by **5**.

cal network formed by pyrite (Figure 8) and has been found in three coordination polymer systems.²⁷

The topological network of **4** and **5** also comprised two different nodes, one ligand-based and one Ag-based, indicating that topologically all ligands were the same, as were all Ag centers. The ligand node was defined as the centroid of the central ring and had the same six links to Ag nodes as those seen for the networks formed by **1–3**, one for each pyridine arm and another for each pair of chelated S atoms. The Ag nodes in turn were again three-connected. The resulting topological network was different to that formed by **1–3**, with ligand nodes having short topological terms of $4^2.6^{10,8^3}$ and Ag nodes having short topological terms of 4.6^2 (Figure 9). Despite the two coordination frameworks being related by a skew, no difference was seen for the short topological terms of these two networks. The uninodal 4.6^2 “net” was recognized by Wells as leading to discrete systems;²⁵ however, it has been found to occur as part of two other more complex network structures, one three-dimensional²⁷ and the other two-dimensional.²⁸ This particular combination of three- and six-connected nodes is also found in the topological network formed by rutile TiO₂ (Figure 9) and has also been seen in a number of other coordination polymeric systems.²⁹

The topological network of **6** comprised two different nodes, one ligand-based and one Ag-based, indicating that topologically all ligands were the same, as were all Ag

(23) (a) Suenaga, Y.; Kuroda-Sowa, T.; Maekawa, M.; Munakata, M. *J. Chem. Soc., Dalton Trans.* **2000**, 3620–3623. (b) Ning, G. L.; Munakata, M.; Wu, L. P.; Maekawa, M.; Kuroda-Sowa, T.; Suenaga, Y.; Sugimoto, K. *Inorg. Chem.* **1999**, *38*, 1376–1377.

(24) For example: (a) Mallik, A. B.; Lee, S.; Lobkovsky, E. B. *Cryst. Growth Des.* **2005**, *5*, 609–616. (b) Li, L.; Fan, J.; Okamura, T.-A.; Li, Y.-Z.; Sun, W.-Y.; Ueyama, N. *Supramol. Chem.* **2004**, *16*, 361–370. (c) Pickering, A. L.; Long, D.-L.; Cronin, L. *Inorg. Chem.* **2004**, *43*, 4953–4961. (d) Fan, J.; Zhu, H.-F.; Okamura, T.-A.; Sun, W.-Y.; Tang, W.-X.; Ueyama, N. *Inorg. Chem.* **2003**, *42*, 158–162. (e) Brooks, N. R.; Blake, A. J.; Champness, N. R.; Cunningham, J. W.; Hubberstey, P.; Teat, S. J.; Wilson, C.; Schröder, M. *J. Chem. Soc., Dalton Trans.* **2001**, 2530–2538.

(25) Wells, A. F. *Three-Dimensional Nets and Polyhedra*; John Wiley and Sons: New York, 1977.

(26) For example: (a) Maspoch, D.; Ruiz-Molina, D.; Wurst, K.; Rovira, C.; Veciana, J. *Chem. Commun.* **2004**, 1164–1165. (b) Du, M.; Guo, Y.-M.; Chen, S.-T.; Bu, X.-H.; Batten, S. R.; Ribas, J.; Kitagawa, S. *Inorg. Chem.* **2004**, *43*, 1287–1293.

(27) (a) Tynan, E.; Jensen, P.; Kelly, N. R.; Kruger, P. E.; Lees, A. C.; Moubaraki, B.; Murray, K. S. *Dalton Trans.* **2004**, 3440–3447. (b) Chae, H. K.; Kim, J.; Delgado, Friedrichs, O.; O’Keeffe, M.; Yaghi, O. M. *Angew. Chem., Int. Ed.* **2003**, *42*, 3907–3909. (c) Batten, S. R.; Hoskins, B. F.; Robson, R. *Angew. Chem., Int. Ed. Engl.* **1995**, *34*, 820–822.

(28) Zhong, J. C.; Munakata, M.; Kuroda-Sowa, T.; Maekawa, M.; Suenaga, Y.; Konaka, H. *Inorg. Chim. Acta* **2001**, *322*, 150–156.

(29) (a) Qin, C.; Wang, X. L.; Wang, E.-B.; Su, Z.-M. *Inorg. Chem.* **2005**, *44*, 7122–7129. (b) Xie, L.; Liu, S.; Gao, B.; Zhang, C.; Sun, C.; Li, D.; Su, Z. *Chem. Commun.* **2005**, 2402–2404. (c) Qin, C.; Wang, X.; Carlucci, L.; Tong, M.; Wang, E.; Hu, C.; Xu, L. *Chem. Commun.* **2004**, 1876–1877. (d) Carlucci, L.; Ciani, G.; Porta, F.; Proserpio, D. M.; Santagostini, L. *Angew. Chem., Int. Ed.* **2002**, *41*, 1907–1911. (e) Jensen, P.; Price, D. J.; Batten, S. R.; Moubaraki, B.; Murray, K. S.; *Chem. Eur. J.* **2000**, *6*, 3186–3195. (f) Batten, S. R.; Hoskins, B. F.; Robson, R. *Inorg. Chem.* **1998**, *37*, 3432–3434. (g) Kim, C.-H.; Iwamoto, T. *Bull. Korean Chem. Soc.* **1997**, *18*, 791–793.

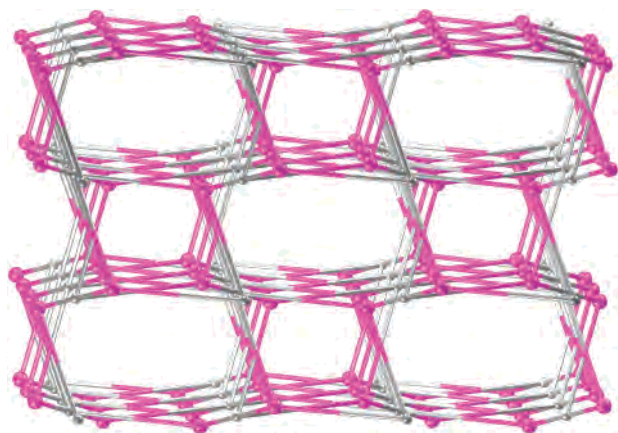


Figure 10. View along the c axis of the three-dimensional topological net formed by **5** illustrating the previously unknown network topology.

centers. The ligand node was defined in the same fashion as the previous ligand nodes and again had links to six Ag nodes, resulting in a ligand node topology of $4^4.6^2.8^7.10^2$. The Ag nodes in turn were three-connected with short topological terms of $4^2.6$ (Figure 10), closely related to the 4.6^2 Ag nodes seen for the topological networks of **4** and **5**. The $4^2.6$ node topology has also been seen previously in five different coordination polymeric systems, two related three-dimensional systems²⁷ and three related one-dimensional polymers that were extended into three dimensions by hydrogen bonding.³⁰ The two three-dimensional polymers showed the closest relationship to **6**, as they also showed six-connected nodes.²⁷ One of these was also seen to have short topological terms of $4^4.6^2.8^8.10$ for its six-connected nodes, very closely related to the $4^4.6^2.8^7.10^2$ nodes seen in **6**. Other than this related topological network, nodes with $4^4.6^2.8^7.10^2$ topology appear to be previously unknown. The topological terms seen for this ligand-based node are very different to those seen for the other **4tet** structures (**4** and **5**) despite the same metal cation and ligand being involved. They are also different to those seen for the **3tet** structures where the ligands adopt similar conformations.

Conclusion

The ligands **3tet** and **4tet** were successfully used to form complexes, some of them showing quite unusual structural features such as the restriction of ligand geometries to two broad categories, the regularity of formation of three-layered π -stacking motifs and the large cavities formed in the complexes of **4tet** in spite of its flexibility. Variations in the solvents used for crystallization and the use of different anions commonly have a significant effect on the overall framework of Ag(I) coordination polymers.^{1,2} However, this was not seen in these six complexes to the extent that would generally have been predicted under the current paradigm. The three structures of **3tet**-containing Ag(I) complexes with different anions were isomorphous. This was unexpected, as the Ag(I) salts involved in forming the complexes, AgClO_4 , PF_6^- , and CF_3CO_2^- , had anions of significantly

different size and coordination ability. Despite these differences, the anions were all held in place in the structure by weak interactions with the ligand, and the same overall nonporous structure resulted. Two of the **4tet**-containing Ag(I) complexes, **4**·**2MeCN**·**2CHCl₃** and **5**·**6MeCN**, were isotopological and structurally very similar. Both of these complexes were more porous than the complexes of **3tet**, with high proportions of the volume of the unit cell occupied by solvent molecules. The complex formed from the reaction of **4tet** and AgCF_3SO_3 , **6**·**3H₂O**, was different than either of the other two **4tet** complexes. The arrangement of the ligand in this complex was similar to that seen in the complexes of **3tet**, and the resulting structure was different than those of **4** or **5**, although it also had a porous structure.

Despite the flexibility of the ligands all of their complexes were found to fit two categories of ligand geometry. These were the complexes, **1**–**3** and **6**·**3H₂O**, where the ligand had all four pyridine arms stretched out approximately in the plane of the central benzene ring (stretched conformation), and the complexes, **4**·**2MeCN**·**2CHCl₃** and **5**·**6MeCN**, that had one pair of para pyridine arms stretched out and the other folded away from the plane of the central ring (folded conformation). This folded conformation was a less extreme version of that seen in the previous complex of the isomeric ligand 1,2,4,5-tetrakis(2-pyridylmethylsulfanylmethyl)benzene, in which the folded pyridine arms were arranged parallel to the central benzene ring to form a three-layered π stack.^{6a} While preorganization of ligands by facial segregation to avoid steric hindrance has been proposed as a means of providing a degree of rigidity to flexible ligands,³ it was not seen to occur in the expected fashion in these six complexes. Despite the expectation that ortho pyridine arms would organize themselves on opposite faces of the central ring the coordination mode adopted in the complexes prevented them from doing so.

The complexes of **3tet** and **4tet** also displayed a number of weaker interactions, both between ligand molecules and also to anions or incorporated solvent molecules. The most commonly seen interaction was the formation of interligand three-layer π -stacks; all complexes except **6**·**3H₂O** displaying this motif. Other interactions between the aromatic rings such as C–H··· π interactions were also observed. Topological analyses of the networks formed by the complexes of **3tet** and **4tet** showed them to all comprise six-connected ligand-based nodes and three-connected metal-based nodes with different short topological terms. Such six-connected, ligand-based nodes are rare among coordination polymers; only four examples having been previously seen.^{4c,d,23} The overall topologies of the cationic frameworks of complexes **1**–**3** were found to be that of the pyrite net, which has been seen only in three previous coordination polymers.²⁷ The overall topologies of the frameworks of **4** and **5** were that of the rutile net which again is not common among coordination polymer architectures.²⁹ The overall topology of the framework of **6** was previously unknown, with only one coordination polymer system showing a closely related topology.^{27a}

Despite the similarity of the two ligands and use of the same metal salts in the preparation of certain complexes,

(30) Pickering, A. L.; Cooper, G. J. T.; Long, D.-L.; Cronin, L. *Polyhedron* **2004**, *23*, 2075–2079.

the resulting structures were found to be both interesting and surprisingly different. The three structures of complexes of **3tet** were isomorphous, nonporous three-dimensional networks, and all three structures of complexes of **4tet** were porous three-dimensional networks, two of which were very similar to each other, the other of which was structurally different.

Acknowledgment. We thank Professor Ward T. Robinson and Dr. Jan Wikaira (University of Canterbury) for X-ray

data collection and the University of Otago Research Committee and the Department of Chemistry, University of Otago for financial support.

Supporting Information Available: X-ray crystallographic file in CIF format for the structure determination of **1–6**; full topological analyses for complexes **1–6**. This material is available free of charge via the Internet at <http://pubs.acs.org>.

IC061867M